Fluorescence Quenching Studies of Apolipoprotein A-I in Solution and in Lipid–Protein Complexes: Protein Dynamics†

William W. Mantulin* and Henry J. Pownall

Division of Atherosclerosis and Lipoprotein Research, Baylor College of Medicine and The Methodist Hospital, Houston, Texas 77030

David M. Jameson

Department of Pharmacology, University of Texas Health Science Center at Dallas, Dallas, Texas 75235

Received December 13, 1985; Revised Manuscript Received August 21, 1986

ABSTRACT: Fluorescence lifetime and intensity quenching studies of human plasma apolipoprotein A-I (apo A-I) in aqueous solution and in recombinant lipoprotein complexes with dimyristoylphosphatidylcholine (DMPC) indicate differences in conformational dynamics. In aqueous solution, the bimolecular quenching constants (k^*) for lipid-free apo A-I fluorescence quenching by oxygen and acrylamide are 2.4×10^9 and 0.38×10^9 M^{-1} s^{-1}, respectively. These values are independent of the oligomeric form of the protein. There is no correlation between the relatively small k^* for apo A-I, which reflects rapid, low-amplitude protein fluctuations, and the labile conformational changes of apo A-I folding reactions, like denaturation, which occur on a slower time scale. In recombinant DMPC/apo A-I complexes (100:1 molar ratio) the protein increases in amphiphilic α-helical structure as it blankets the lipid matrix. The apparent k^* for oxygen quenching of apo A-I fluorescence in the complex is large and increases in a temperature-dependent manner. We have introduced a two-compartment model, which discriminates the source of quencher molecules as aqueous or lipid, to describe oxygen quenching of DMPC/apo A-I fluorescence. The magnitude and temperature dependence of the apparent k^* predominantly reflect the partitioning of oxygen between the two phases rather than being a probe of the lipid physical state. Calculations of the helical hydrophobic moment in apo A-I indicate that tryptophan residues 8 and 72 occur at the lipid–protein interface of amphiphilic α-helices, whereas the other two tryptophan residues (50, 108) lie on the nonpolar faces of amphiphilic helices. This placement of fluorescent residues, relative to the lipid–protein interface, suggests a temperature-dependent solvation barrier for oxygen quencher molecules originating in the lipid phase. The diminution of the temperature dependence of the oxygen quenching efficiency of DMPC/apo A-I fluorescence by the addition of sucrose, which perturbs the water–phospholipid–protein interfacial region, probably reflects changes in the solvation barrier. Quenching of DMPC/apo A-I intrinsic fluorescence by acrylamide is similar to that observed for lipid-free apo A-I. Analysis of this data does not require a two-compartment model. The acrylamide quenching results indicate that the increase in α-helical structure, experienced by apo A-I in lipid association, does not significantly alter the access of uncharged quenchers to fluorescent residues. Our studies demonstrate that the hydrated lipid–protein interface of lipoproteins is the major factor in regulating protein dynamics.

Apolipoprotein A-I (apo A-I)[1] is the major protein constituent of human plasma high-density lipoprotein (HDL). In addition to stabilizing HDL architecture, apo A-I activates the enzyme lecithin:cholesterol acyltransferase, which catalyzes the formation of cholesteryl esters in the plasma (Soutar et al., 1975). Apo A-I has a molecular weight of 27 800, and its sequence of 243 amino acid residues is known (Baker et al., 1974; Brewer et al., 1978). Apo A-I spontaneously associates with synthetic phospholipids (Pownall et al., 1978) or through detergent-mediated recombination (Matz & Jonas, 1982) to form well-characterized discoidal complexes (Brouillette et al., 1984). Conformational studies indicate that apo A-I possesses a remarkable degree of structural adaptability manifested by (1) a low free energy of denaturation ΔG − 2 kcal/mol (Tall et al., 1976; Mantulin & Pownall, 1985), (2) a large increase in α-helical content (to 85%) upon association with lipid (Morrisett et al., 1977), and (3) variations in secondary structure for different oligomeric forms (Edelstein & Scanu, 1980). Segrest et al. (1974) proposed that the apolipoproteins bind at a lipid interface through formation of multiple amphiphilic helical structures in which the nonpolar helical face inserts into the hydrophobic phospholipid environment. Unfortunately, no X-ray crystallographic data, describing the three-dimensional orientation of apo A-I, is available to confirm the amphiphilic helix structure. Eisenberg et al. (1982), however, developed an algorithm, the helical hydrophobic moment, which can be used to predict the location of amphiphilic helical sequences of interfacial proteins, including plasma apolipoproteins (Pownall et al., 1983; Krebs & Phillips, 1983). A high helical hydrophobic moment represents a qualitative measure of the amphiphilicity of a given

† This research was supported by grants from the National Institutes of Health (HL27104 to W.W.M. and HL27341 to H.J.P.) and the Robert A. Welch Foundation (I-986 to D.M.J. and Q-906 to H.J.P.).

* Address correspondence to this author.

[1] Abbreviations: apo A-I, apolipoprotein A-I; apo C-I, apolipoprotein C-I; apo C-II, apolipoprotein C-II; DMPC, dimyristoylphosphatidylcholine; DPH, 1,6-diphenyl-1,3,5-hexatriene; HDL, high-density lipoprotein; Prodan, 6-propionyl-2-(dimethylamino)naphthalene; EDTA, ethylenediaminetetraacetic acid; Tris, tris(hydroxymethyl)aminomethane.

0006-2960/86/0425-8034$01.50/0

apolipoprotein. The fluorescent tryptophan residues of apo A-I occur in helical regions that also show a high helical hydrophobic moment. This predicted tryptophan location serves as a basis of the present paper.

The literature of fluorescence quenching studies in lipoproteins is extensive [for a review see Mantulin and Pownall (1983)]; however, only recent studies have included time-resolved methods. Using oppositely charged quenchers iodide and pyridium ions, Pownall and Smith (1974) showed that apparent Stern–Volmer quenching constants (K_{sv}) for apo A-I intrinsic fluorescence are 20–30% lower when compared to those for aqueous tryptophan. They attributed this effect to shielding by the protein's secondary and tertiary structure. Self-association and association with phospholipid further decreased the fluorescence quenching efficiency for the apo A-I. Similar results have been obtained for apolipoproteins C-I (Jackson et al., 1974; Jonas et al., 1982), C-III (Pownall & Smith, 1974), and A-IV (Weinberg & Spector, 1985). Unfolding of apolipoprotein secondary structure increases the apparent K_{sv} for both charged (iodide ion) and neutral (acrylamide) quenchers in apolipoproteins A-I (Rosseneu et al., 1982), C-II (Mantulin et al., 1980), and A-IV (Dvorin et al., 1985), but not to the levels of the fluorophore free in aqueous solution. Maliwal et al. (1985) measured the time-resolved oxygen quenching of apo C-I and apo C-II fluorescence (both are single tryptophan containing apolipoproteins) and concluded that the tryptophan residues are located near the surface of the protein, since the quenching constants are about 60% of diffusion limits. Association with lipid (DMPC or sodium dodecyl sulfate) increased the apparent quenching constant approximately 5-fold, but the authors did not resolve the uncertainty arising from the higher oxygen concentration in the lipid phase. Fluorescence lifetime resolved anisotropy measurements in the recombinant complexes showed temperature-dependent quenching constants and significant tryptophan motional freedom for both apo C-I and apo C-II, indicating the influence of lipid fluidity on protein dynamics.

In the present study, we examine the conformational dynamics of apo A-I in aqueous buffer and in association with dimyristoylphosphatidylcholine (DMPC) using the technique of fluorescence lifetime and intensity quenching [for a review see Eftink and Ghiron (1981)]. On the basis of these measurements and the helical hydrophobic moment calculations, we examine the following problems: (1) In a lipid-free form is there a correlation between the low free energy of apo A-I denaturation and its structural flexibility on a nanosecond time scale? (2) Does the increased helical content of apo A-I, resulting from association with phospholipid, account for changes in protein fluorescence quenching patterns? (3) Can we devise a model for apolipoprotein fluorescence quenching in the presence of lipid? (4) Is the lipid–protein interface important for understanding apo A-I structural dynamics in lipoproteins? (5) What is the amphiphilic helix orientation relative to the lipid surface?

Experimental Procedures

Materials. DMPC was purchased from Calbiochem (La-Jolla, CA). Apo A-I was purified as previously described (Pownall et al., 1978), and the DMPC/apo A-I recombinant complexes (model HDL) were formed by spontaneous association of the components in an incubation mixture at the DMPC transition temperature (T_c, 24 °C) (Pownall et al., 1981a). The average lipid to protein molar ratio in the model HDL was 100:1. Apo A-I concentrations were determined by absorption spectroscopy (1 mg/mL = 1.1 *A* units at 280 nm) (Edelhoch, 1967), and DMPC concentrations were calculated from the phosphorus assay of Bartlett (1959). Electrophoresis-grade acrylamide from Bio-Rad Laboratories (Richmond, Ca) contributed no fluorescence signal under our experimental conditions and was used without further purification. 1,6-Diphenyl-1,3,5-hexatriene (DPH) and 6-propionyl-2-(dimethylamino)naphthalene (Prodan) were purchased from Molecular Probes (Junction City, OR). DPH and Prodan incorporation into model HDL was previously described (Mantulin et al., 1981). A standard buffer composed of 0.1 M NaCl, 1 mM NaN_3, 1 mM EDTA, and 10 mM Tris, pH 7.4, was used throughout.

Fluorescence Spectroscopy. Fluorescence lifetimes were measured on an SLM Instruments (Urbana, IL) Model 4800. The emission was observed through a Corning 0-52 filter. The excitation wavelength (295 nm) preferentially excites tryptophan residues. At this wavelength the absorbance of our solutions was less than 0.05, unless otherwise indicated. For intensity-based quenching measurements with acrylamide, a correction factor was applied to compensate for attenuation of excitation light intensity (Parker, 1968) by acrylamide (ϵ_{295} = 0.23). A modulation frequency of 18 MHz was employed to measure the phase shift and calculate the fluorescence lifetime. Steady-state intensity and fluorescence spectra were recorded on a Model 8000 fluorometer (SLM Instruments). Oxygen quenching studies were performed in a stainless steel high-pressure chamber with optical ports, which was originally described by Lakowicz and Weber (1973). The sample quartz cuvette was 2 × 2 cm to facilitate rapid equilibration of the oxygen gas phase atmosphere with the magnetically stirred sample. After equilibration the oxygen concentration was calculated from standard solubility tables (Washburn, 1928).

Data Analysis. The criterion for dynamic fluorescence quenching in a homogeneous phase is a concurrent decrease in fluorescence lifetime and intensity according to the Stern–Volmer equation:

$$F_0/F = \tau_0/\tau = 1 + K_{sv}[Q] = 1 + k^*\tau_0[Q] \qquad (1)$$

where F_0 and F are the unquenched and quenched fluorescence intensity, respectively, and τ_0 and τ correspond to the fluorescence lifetime in the absence and presence of a quencher concentration [Q]. The Stern–Volmer quenching constant (K_{sv}) is the product of the unquenched fluorescence lifetime and the bimolecular quenching constant (k^*). Deviations from linearity in the fluorescence intensity plots may be interpreted in terms of a static quenching component. In addition, eq 1 can be amended to include the effect of lifetime heterogeneity arising from multiple emitting loci or intrinsically complex intensity decay kinetics (Eftink & Jameson, 1982). Since our lifetime quenching data was collected at a single modulation frequency (18 MHz), we are unable to provide a resolution of the effects of heterogeneity in the emission of apo A-I, and we calculate k^* from eq 1 with τ_0 measured at 18 MHz. In recombinant HDL a lipid–protein interface forms and fluorescent tryptophan residues of apo A-I are quenched by diffusing molecules, originating from either the lipid phase or the surrounding aqueous milieu, and as such the protein experiences a quencher concentration gradient that is simply the partition coefficient (K) of the quencher between the two phases. Not only are the quencher concentrations in the lipid and water phases different, but the bimolecular quenching constants also differ. Implicit in our model are the assumptions that, regardless of lipid or aqueous phase, (1) quenching is primarily through isotropic, diffusion-controlled events, and (2) all quencher–fluorophore collisions result in deactivation. Figure 1 contains a diagram of the various deactivation rate processes of an excited-state fluorophore (F*). Under con-

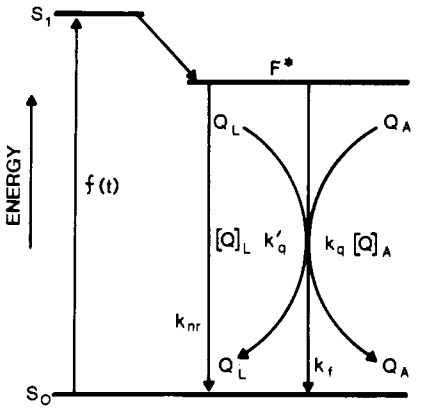

FIGURE 1: Deactivation rate processes for an excited-state fluorophore (F*).

tinuous illumination from a constant excitation function [$f(t)$], F* is depopulated by radiationless (k_{nr}) or fluorescence (k_f) mechanisms in the absence of quenchers.

$$d[F^*]/dt = f(t) - (k_{nr} + k_f)[F^*] \quad (2)$$

By definition $(k_{nr} + k_f)^{-1}$ is equal to τ_0, the fluorescence lifetime in the absence of quenching, which is not to be confused with the natural lifetime $(1/k_f)$. Under quenching conditions, including both aqueous and lipid-phase events (Figure 1)

$$d[F^*]/dt = f(t) - (k_{nr} + k_f + k_q[Q]_A + k'_q[Q]_L)[F^*] \quad (3)$$

where $[Q]_A$ and $[Q]_L$ are the quencher concentration in the aqueous and lipid phases, respectively, and k_q and k'_q correspond to the bimolecular quenching constants in those phases. Using the mathematical formalism for the steady-state solution of deactivation processes supplied by Vaughan and Weber (1970) in the Appendix to their paper, we obtain

$$F_0/F = (1 + \tau_0 k_q[Q]_A)(1 + \tau_0 k'_q[Q]_L) \quad (4)$$

Eq 4 can be rearranged to include the partition coefficient ($K = [Q]_L/[Q]_A$), and at low quencher concentration

$$F_0/F = 1 + (Kk'_q + k_q)[Q]_A\tau_0 \quad (5)$$

An alternative derivation, which arises from definitions of deactivation processes in the fluorescence lifetime mode (Figure 1), yields

$$1/\tau = k_{nr} + k_f + k_q[Q]_A + k'_q[Q]_L \quad (6)$$

and

$$\tau_0/\tau = (k_{nr} + k_f + k_q[Q]_A + k'_q[Q]_L)/(k_f + k_{nr}) \quad (7a)$$

$$\tau_0/\tau = 1 + (Kk'_q + k_q)[Q]_A\tau_0 \quad (7b)$$

RESULTS

The fluorescence lifetime and intensity quenching plots of tryptophan by oxygen are collinear (in standard buffer at 25 °C), indicating dynamic quenching processes, and the calculated (from eq 1) bimolecular quenching constant is $k^* = 11.3 \times 10^9$ M^{-1} s^{-1} (Table I) in good agreement with published data (Lakowicz & Weber, 1973). The calculated bimolecular quenching constant for tryptophan fluorescence by acrylamide is less ($k^* = 6.6 \times 10^9$ M^{-1} s^{-1}) than that for oxygen, and the intensity quenching plot exhibits slight positive curvature in agreement with the observations of Eftink and Ghiron (1976).

Figures 2 and 3 present fluorescence lifetime and intensity quenching data for apo A-I by oxygen and acrylamide, at different protein concentrations. These concentrations encompass predominantly monomeric (less than 0.05 mg/mL) and oligomeric (greater than 0.05 mg/mL) forms of apo A-I

Table I: Fluorescence Quenching Parameters of Apo A-I

sample	quencher	conditions	τ_0 (ns)[c]	k^* (10^9 M^{-1} s^{-1})
tryptophan	oxygen	25 °C	2.9	11.3[a]
	acrylamide	25 °C	2.8	6.6[a]
apo A-I	oxygen	1.2 mg/mL	3.7	2.3[a]
		0.02 mg/mL	3.6	2.4[a]
		40% sucrose	3.3	1.5[a]
	acrylamide	1 mg/mL	3.4	0.43[a]
		0.04 mg/mL	3.3	0.38[a]
DMPC/apo A-I (100:1)	oxygen	33 °C	4.0	10.5[b]
		26 °C	4.1	5.2[b]
		20 °C	4.4	3.7[b]
		33 °C, 40% sucrose	4.1	5.2[b]
		20 °C, 40% sucrose	4.4	4.2[b]
	acrylamide	33 °C	4.1	0.36[a]
		26 °C	4.2	0.28[a]
		20 °C	4.3	0.18[a]

[a] Calculated from eq 1 by using the fluorescence lifetime data. [b] Calculated from eq 7. [c] Measured at 18 MHz by a phase shift method.

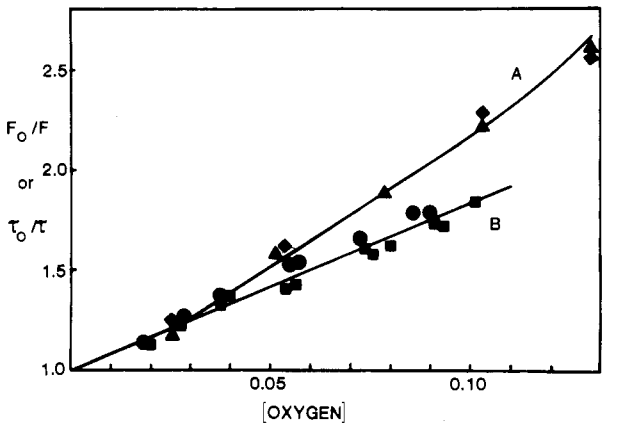

FIGURE 2: Oxygen-based fluorescence quenching from intensity (trace A) and lifetime (trace B) measurements of lipid-free apo A-I in standard buffer at 25 °C. The various closed symbols correspond to different concentrations of apo A-I: 1.2 (◆, ■) and 0.02 mg/mL (▲, ●). The oxygen concentration on the abscissa is in moles per liter.

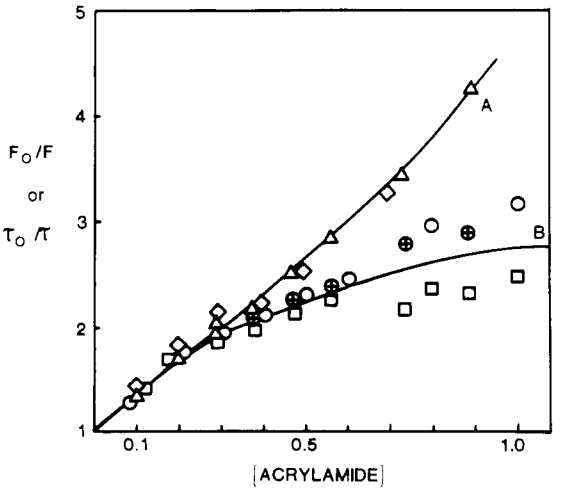

FIGURE 3: Acrylamide-based fluorescence quenching from intensity (trace A) and lifetime measurements (trace B) of lipid-free apo A-I in standard buffer at 25 °C. The various open symbols refer to different concentrations of apo A-I: I 1 (◇, □), 0.4 (⊕), and 0.04 mg/mL (△, ○). The acrylamide concentration on the abscissa is in moles per liter. Other conditions are as in Figure 2.

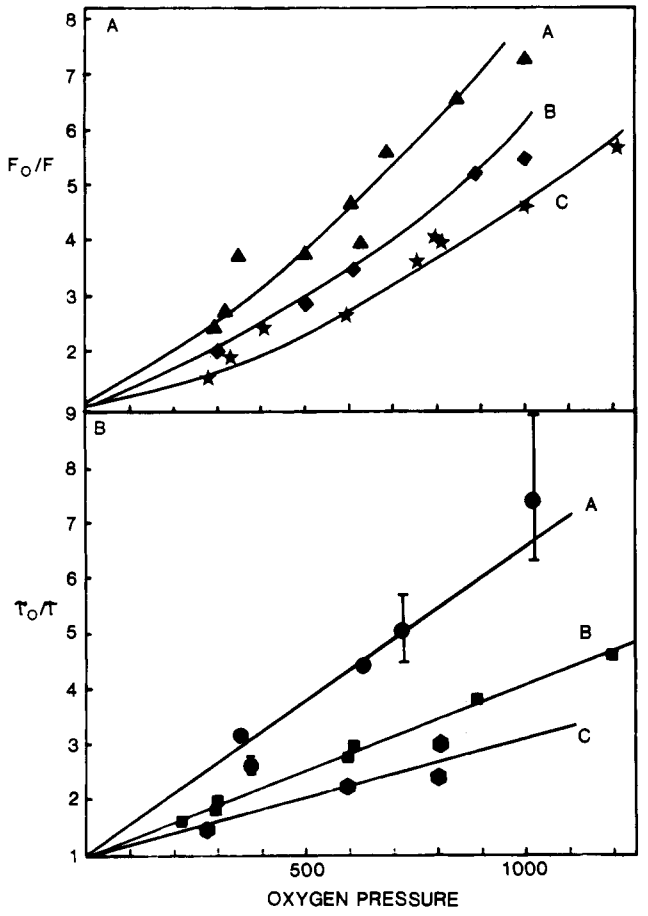

FIGURE 4: Temperature-dependent quenching of DMPC/apo A-I recombinant HDL fluorescence by oxygen. Panel A presents the fluorescence intensity quenching data at 33 (A), 26 (B), and 20 °C (C). Panel B shows the fluorescence lifetime quenching data for the same temperatures: 33 (A), 26 (B), 20 °C (C). The error bars in panel B, trace A, are calculated on the basis of a 100-ps systematic error. The oxygen pressure on the abscissa is presented in psi. Other conditions are as in Figure 2.

(Edelstein & Scanu, 1980). For fluorescence lifetime quenching by oxygen (Figure 2, trace B), we could detect no changes in the bimolecular quenching constant as a function of the degree of association of apo A-I (Table I). Regardless of the degree of self-association in apo A-I, the k^* values are less than for tryptophan in solution, suggesting that the secondary and tertiary structure of the protein shields the fluorescent residues. The linearity of the quenching data over a wide quencher concentration suggests that all the emitting tryptophan residues in apo A-I are accessible to the oxygen, even though the emission maximum (λ_{max} = 339 nm) is blue-shifted relative to tryptophan in solution (λ_{max} = 355 nm). In general, the emission maxima of proteins reflect the extent of tryptophan exposure to solvent water; however, the protein–water interface (in a lipid-free aqueous environment) does not impose a diffusion barrier to oxygen; i.e., there is no correlation between protein emission maxima and bimolecular quenching constants for oxygen-based fluorescence quenching (Lakowicz, 1982). The upward curvature of the intensity-based Stern–Volmer plots (Figure 2, trace A) indicates a possible static component to the quenching process. In the case of fluorescence lifetime quenching by acrylamide (Figure 3, trace B), the state of aggregation again has little influence on the quenching efficiency, which is less than that for oxygen (Table I). The leveling of the lifetime quenching plots at higher acrylamide concentrations suggests that the fluorescent tryptophan residues in apo A-I are not equally accessible to

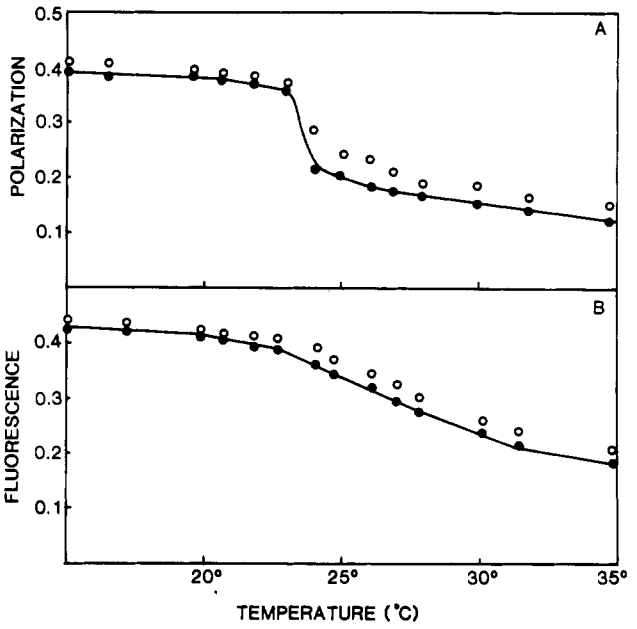

FIGURE 5: Temperature-dependent fluorescence polarization of DPH in multilamellar DMPC liposomes (panel A) and DMPC/apo A-I complexes (panel B). The open circles refer to data collected in 40% sucrose, whereas the closed circles correspond to standard buffer in the absence of sucrose. The excitation wavelength was 360 nm, and the emission was collected through a Corning 3-144 filter.

acrylamide. The steep slope of the intensity quenching plots (Figure 3, trace A) is indicative of static quenching and/or of a heterogeneous emission pattern. At present, this is beyond our ability to resolve with this data set.

Figure 4 shows the fluorescence quenching of DMPC/apo A-I recombinant complexes by oxygen at 33 (A), 26 (B), and 20 °C (C). These temperatures correspond to values above, at, and below the phase transition temperature (T_c) of the complex, as determined by differential scanning calorimetry (Tall et al., 1977) or fluorescence polarization of the lipophilic probe diphenylhexatriene (DPH) (Figure 5) (Mantulin et al., 1981). Both the calorimetric and spectroscopic observations confirm that the association of apo A-I with DMPC broadens the phase transition and raises the lipid T_c. The apparent quenching of DMPC/apo A-I intrinsic fluorescence (Figure 4) is higher at the elevated temperatures and in all cases is larger than for the lipid-free protein (Figure 2). The quenching data in Figure 4 are plotted in terms of oxygen pressure to avoid ambiguities in the relationship between oxygen pressure and concentration. The error bars in Figure 4 (panel B, trace A), calculated on the basis of a systematic error of 100 ps, are included to demonstrate that the relative error in lifetime quenching experiments increases with the extent of quenching. The apparent quenching constants, containing all the bracketed terms in eq 7b, are listed in Table I. At the various temperatures (T = 20, 26, 33 °C)

$$k^*_{app} = K(T)k'_q(T) + k_q(T) \quad (8)$$

In the temperature range of 20 to 33 °C, we observed a constant k^* for apo A-I fluorescence quenching by oxygen in aqueous solution and an invariant UV circular dichroic spectrum (Reijngoud & Phillips, 1984). A reasonable assumption would be that the same pattern will hold for DMPC/apo A-I complexes, namely, that k_q (33 °C) = k_q (26 °C) = k_q (20 °C) = constant. The fact that the gross conformation, as measured by UV circular dichroic spectroscopy, of apo A-I in the recombinant HDL complex is invariant between 20 and 33 °C supports this assumption (data not

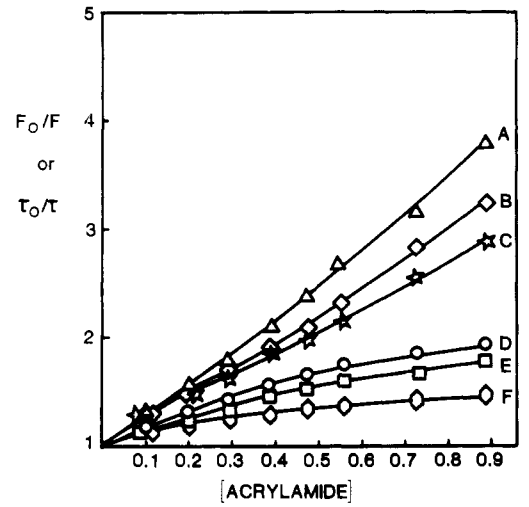

FIGURE 6: Temperature-dependent quenching of DMPC/apo A-I complex fluorescence by acrylamide. Traces A–C correspond to intensity quenching, and traces D–F refer to lifetime quenching. The temperature nomenclature follows: 33 (traces A and D), 26 (traces B and E), and 20 °C (Traces C and F). The acrylamide concentration on the abscissa is in moles per liter. Other conditions are as in Figure 2.

shown). However, because apo A-I is more helical in the complex (Morrisett et al., 1977), we cannot assume that the value of k^*, corresponding to the protein in aqueous solution, is appropriate for k_q. The temperature dependence of the average partition coefficient (K) for oxygen between water and the hydrogen region of the DMPC bilayer has been determined by spin-label oximetry (Subczynski & Hyde, 1983). These values are $K_{33} = 2.8$, $K_{26} = 1.5$–2.5, and $K_{20} = 1.2$; the range of values in K_{26} corresponds to the discontinuity arising at the lipid phase transition. We realize that there is an oxygen concentration gradient from the hydrocarbon region to the head group of the phospholipid matrix, and thus we stress that K is an average value (Peters & Kimmich, 1978). Presumably, the lipid-phase diffusion coefficients k'_q in eq 8 are also temperature-dependent (Subczynski & Hyde, 1984). Since we have no independent measure of the temperature-dependent k'_q (lipid phase) or k_q (aqueous phase), we cannot uniquely solve eq 8. The slightly increased fluorescence quenching efficiency apparent in the intensity plots (Figure 4, panel A) may arise from a static quenching component and/or emission lifetime heterogeneity. The much larger apparent bimolecular quenching constants in the complexes, relative to apo A-I in solution, however, almost certainly reflect the preferential solubility of oxygen in lipid over water.

To further delineate the relationship between $k_q(T)$ and $k'_q(T)$ (eq 8), we altered the viscosity of the aqueous phase by adding sucrose. For example, addition of 40% sucrose to globular protein solutions increases bulk viscosity 6-fold and decreases quencher diffusion rates into and through the protein (Jameson et al., 1984). For apo A-I in solution, the increased viscosity due to 40% sucrose reduces the apparent bimolecular quenching constant by 40%, relative to that observed in the absence of sucrose (Table I). This observation follows the trend detected in hemoglobin and myoglobin by Jameson et al. (1984). For apo A-I fluorescence quenching in the lipid complex (Table I), the addition of 40% sucrose removes the strong temperature dependence of the apparent bimolecular quenching constant, observed in the absence of sucrose. What effect does sucrose exert on the bulk phospholipid and protein and interfacial regions in the recombinant HDL? On the basis of our DPH fluorescence polarization data in Figure 6, we conclude that sucrose generates a slight perturbation of the

Table II: Fluorescence Properties of Prodan in Recombinant DMPC/Apo A-I Complexes

temperature[a]	fluorescence	buffer	40% sucrose
20	λ^b	436	435
	$\Delta\nu_{1/2}{}^c$	3982	3923
26	λ	437	436
	$\Delta\nu_{1/2}$	5181	4848
33	λ	495	484
	$\Delta\nu_{1/2}$	5473	5768

[a] Temperature in °C. [b] Wavelength of maximum emission in nanometers. [c] Spectral width at half-maximum intensity in cm^{-1}.

bulk phospholipid in the DMPC/apo A-I complex. Differential scanning calorimetry of phospholipids (Chowdry et al., 1984) shows that sucrose slightly elevates the temperature of the phase transition (in agreement with Figure 5) and decreases the calorimetric enthalpy of the gel to liquid-crystalline phase transition. Furthermore, sucrose does not significantly alter the helical content of apo A-I in solution or in a phospholipid complex, as calculated from circular dichroic spectra (data not shown). The environmentally sensitive fluorescence probe Prodan (Weber & Farris, 1979) reflects temperature-dependent changes in interfacial polarity in DMPC/apo A-I complexes [Massey et al. (1985) and Table II]. At higher temperatures the hydration of the lipid–water interface increases, as evidenced by the red shift in the emission maximum wavelength [Massey et al. (1985) and Table II]. At 26 and 33 °C the large spectral width at half-maximal intensity indicates heterogeneity in Prodan's microenvironment (Table II). The addition of 40% sucrose to the recombinant HDL reduces the hydration of the interfacial region as measured by Prodan fluorescence (Table II). This observation is consistent with the mild dehydration of phospholipid membranes induced by sucrose (MacDonald, 1985). The properties of the interfacial region between apo A-I amphiphilic helical segments and the phospholipid bilayer are reflected in the average fluorescence properties of the four tryptophan residues in apo A-I. In both standard buffer and 40% sucrose the fluorescence spectrum of apo A-I in DMPC/apo A-I complexes slightly red shifts (330 to 331 nm) between 20 and 30 °C. The solubility of oxygen in the lipid compartment of DMPC/apo A-I complexes does not change with the addition of sucrose, since it is in direct equilibrium with the pressurized oxygen atmosphere. The aqueous solubility of oxygen is reduced by sucrose (Jameson et al., 1984), and therefore the partition coefficient of oxygen between the lipid and aqueous phases increases (K^s) upon the addition of sucrose. Considered together, these data indicate that the normalization in the temperature dependence of the apparent k^* for apo A-I fluorescence quenching in DMPC/apo A-I complexes occurs, in part, because in the presence of sucrose aqueous viscosity increases and k_q is reduced to k_q^s, whereas k'_q remains essentially unchanged. Thus, sucrose addition primarily affects quenching events by altering interfacial properties, rather than protein or lipid dynamics.

The temperature-dependent fluorescence quenching in the DMPC/apo A-I complexes by acrylamide (Figure 6) is analyzed according to eq 1, since acrylamide is essentially insoluble in the lipid phase. The apparent bimolecular quenching constants are 20–30 times less than those for the corresponding cases for quenching by oxygen (Table I). In addition, the lipid shields the tryptophan residues from acrylamide, and the lifetime-based quenching efficiency (Figure 6, traces D–F) is less than that for apo A-I free in solution (Figure 3, trace B). The lifetime quenching efficiency levels off at 33, 26, and 20 °C. This result demonstrates that a fraction of apo A-I fluorophores are not accessible to quencher regardless of the

helical structure of the protein. The acrylamide-based fluorescence intensity quenching plots for apo A-I in solution (Figure 3, trace A) or in recombinant lipid complex (Figure 6, traces A–C) are similar and show a slight upward curvature, suggestive of static quenching.

Discussion

Our purpose in undertaking these experiments was to gain insight into the conformational dynamics of human plasma apolipoprotein A-I by measuring the quenching of apo A-I intrinsic fluorescence. To expand the scope of our study, we contrasted the fluorescence quenching patterns for two very different quenchers: highly effective oxygen, which is a small, nonpolar, and uncharged molecule, and the less effective acrylamide, a larger, polar, and also uncharged molecule. Lakowicz and Weber (1973) provided experimental evidence that oxygen quenching of intrinsic protein fluorescence (i.e., from tryptophanyl residues) was consistent with a dynamic collisional mechanism and reflected protein structural fluctuations on a nanosecond time scale. That is, random, rapid, small-displacement fluctuations of the average conformation provide a dynamic access channel for the oxygen quencher to reach the tryptophan residues in the protein. Unlike oxygen, which quenches all fluorescent residues, acrylamide may selectively quench fluorescence of exposed tryptophan residues in proteins. For example, Eftink and Jameson (1982) showed that, in liver alcohol dehydrogenase, oxygen quenched the fluorescence of both the exposed (15) and buried (314) tryptophan residues, albeit with significantly different quenching constants, whereas acrylamide only quenched the solvent-exposed residue. A comparison of the relative quenching efficiencies of the different quenchers can thus provide information about protein topography and accessibility of domain structures.

Fluorescence Quenching of Apo A-I in Solution. In aqueous solution that is lipid-free, apo A-I assumes a conformation high in α-helical content (67%) (Morrisett et al., 1977). This conformation is probably not a unique three-dimensional structure but rather an average value, since apolipoprotein structure often reflects the history of the sample. Our apo A-I fluorescence lifetime and intensity quenching data indicate that even though the forces maintaining a native conformation in apo A-I are small, the quenching processes are relatively inefficient (Table I), when compared with multi-tryptophan-containing globular proteins (Lakowicz, 1982) or apo C-I (Jonas et al., 1982) and apo C-II (Maliwal et al., 1985). From Table I the bimolecular quenching constants (k^*) for quenching of apo A-I fluorescence by oxygen and acrylamide are 2.3×10^9 and 0.4×10^9 M^{-1} s^{-1}, respectively, whereas in most multi-tryptophan-containing proteins the corresponding values range from 2.0×10^9 to 5.4×10^9 M^{-1} s^{-1} for oxygen quenching (Lakowicz, 1982) and from 0.1×10^9 to 2.7×10^9 M^{-1} s^{-1} for acrylamide (Eftink & Ghiron, 1976). Both apo C-I and apo C-II are single tryptophan containing apolipoproteins, which are approximately one-third as large as apo A-I and contain less α-helical structure than apo A-I (apo C-I, 57% α-helix; apo C-II, 23% α-helix; Morrisett et al., 1977). Since α-helices are relatively rigid structures, the combination of high helical content (and the unknown tertiary structure of apo A-I) coupled with a larger molecular weight (favoring shielding) may account for the 2-fold difference in the k^* (Table I) between apo A-I and the apo C proteins (Maliwal et al., 1985). The independence of apo A-I quenching parameters (for both oxygen and acrylamide) on the degree of self-association (Table I) or temperature (between 20 and 30 °C) is probably linked to the intrinsic barrier to quenching in the monomeric and folded native protein. Our quenching studies suggest that the dynamic aspects of apolipoproteins responsible for diffusion of oxygen or acrylamide into the protein matrix are not equivalent between apo A-I and apo C, even though the energetics of gross conformational change (e.g., denaturation) are similar in the different proteins (Tall et al., 1976; Mantulin et al., 1985, 1980). Since our time-resolved quenching measurements are performed at only one modulation frequency (18 MHz), our apparent bimolecular quenching constants (k^*) represent an average rate of quenching for all emitting tryptophan residues in apo A-I. Detailed analysis of fluorescence quenching at individual tryptophan residues in such a complex system is probably outside the resolution of present time domain techniques (Gratton & Limkeman, 1983; Beechem & Brand, 1985); however, determination of different tryptophan classes (environment) may be possible.

Fluorescence Quenching of Apo A-I in Recombinant HDL. When apo A-I spontaneously associates with DMPC to form a recombinant HDL-like particle, the α-helical content increases from about 67% to 86% (Morrisett et al., 1977; Scanu et al., 1982). This kinetically controlled association event (Pownall et al., 1978) stabilizes the HDL recombinant bilayer particle by arranging the amphiphilic helices of apo A-I such that the polar residues face the aqueous milieu and the nonpolar residues insert into the phospholipid surface (Segrest et al., 1974), thereby forming a lipid–protein interface at the cylindrical face of the helix. These recombinant HDL are bilayer disks with protein on the perimeter (Brouillette et al., 1984). Our fluorescence quenching data (by oxygen) for the DMPC/apo A-I complexes (Figure 5) show an apparent increase in efficiency, compared to quenching of apo A-I fluorescence. This increased efficiency of quenching, coupled to the blue shift of the fluorescence (Morrisett et al., 1977) upon lipid binding, suggests that the tryptophan residues of apo A-I are intimately involved with the lipid phase. Our quenching data (Figure 5, panel B) also show a temperature dependence relative to the phase state of DMPC; that is, apparent bimolecular quenching constants are larger for liquid-crystalline DMPC/apo A-I complexes ($T > T_c$). We have introduced a two-compartment model to describe the relationship between the measured apparent bimolecular quenching constant (k^*) and the quenching constants in the aqueous (k_q) and lipid (k'_q) phases (eq 8). The proportionality constant is the temperature-dependent oxygen partition coefficient (K), measured by spin-label oximetry (Subczynski & Hyde, 1983). Since k^* (eq 1) for apo A-I quenching by oxygen (in aqueous solution) is independent of temperature between 20 and 33 °C and there is no change in the ellipticity of DMPC/apo A-I in the same temperature interval, we assume that k_q becomes a constant independent of temperature. We have no independent measure of the true value of k_q, nor of any temperature dependence of k'_q, and thus we cannot uniquely solve eq 8 for k'_q. However, examination of eq 8 allows the conclusion that the temperature dependence of k^*_{app} predominantly reflects the partition of oxygen between the two phases rather than being a probe of the lipid physical state. Even though the oxygen quenching data of Maliwal et al. (1985) for DMPC/apo C-I and DMPC/apo C-II recombinant complexes cover a larger temperature range (5–40 °C) than our work, we applied the formalism of eq 8 to their data (their Table II) with the additional assumption that k_q is approximately equal to the quenching rate for the corresponding apolipoprotein in a lipid-free state. This general analysis suggests that not only is k^*_{app} largely dependent on the oxygen

partition coefficient but also that the value of $k'_q(T)$ is substantially larger for apo C than for apo A-I. It is unlikely that $k'_q(T)$ differs by an order of magnitude between apo A-I and apo C/DMPC recombinant complexes, and thus an apparent difference in the nature of the protein–phospholipid interface must exist, as we shall discuss in the next section.

By contrast, our acrylamide fluorescence quenching data show a limited temperature dependence in the DMPC/apo A-I complexes (Figure 6) and a slight reduction in efficiency relative to quenching in the absence of phospholipid (Table I). Since acrylamide is poorly soluble in nonpolar solvents, we applied eq 1 to calculate the apparent k^* and considered only aqueous origins for the diffusing quencher (including both the bulk aqueous phase and the water-containing interfacial region). The acrylamide quenching data suggests that the increase in α-helical content experienced by apo A-I upon association with DMPC does not substantially alter the ability of uncharged quenchers to access the tryptophan residues of the protein. The apparent temperature dependence of quenching shows that acrylamide is probing some subtle difference in the physical state of apo A-I (structural or dynamic) even though gross conformational changes are not evident from the UV circular dichroic spectra over the same temperature range. However, the tapering off of the fluorescence lifetime quenching plots (Figure 6, traces D–F) indicates a selective shielding effect to dynamic quenching imposed by the presence of DMPC (compare to Figure 3, trace B). Association of apo A-I with DMPC does not, however, strongly perturb the acrylamide fluorescence intensity quenching curves, indicating that the important static quenching mechanism remains functional in the protein–lipid interfacial region.

The Interface between DMPC and Apo A-I. The amphiphilic helix model of apolipoprotein structure, introduced by Segrest et al. (1974), makes the phospholipid–water interface the prime target for surface-active (interfacial) proteins such as apo A-I. The polarity or hydration of the phospholipid–water interface may in fact regulate the association of apolipoproteins with phospholipid (Pownall et al., 1981b). For a phospholipid in the liquid-crystalline state the polarity of the lipid–water interface resembles that of alcohol (Zachariasse et al., 1981) and the extent of hydration is greater than in the gel state (Watts et al., 1978). Employing environment-sensitive fluorescence probes, Massey et al. (1985) demonstrated that the water–phospholipid interfacial region of DMPC/apo A-I discoidal recombinant HDL contains substantial amounts of bound water and that the level of hydration increases when the bulk lipid (DMPC) melts (Table II). Prodan senses the same interfacial environment in DMPC single-bilayer vesicles and recombinant DMPC/apo A-I complexes [Massey et al. (1985) and their Figure 3]. Our quenching experiments monitor both the dynamics and access of quenchers to the tryptophan residues in helical segments of apo A-I. Several lines of evidence indicate that these tryptophan residues occur at the interface. The fluorescence maximum of the intrinsic emission from DMPC/apo A-I complexes occurs at 331 nm, which is blue-shifted relative to apo A-I fluorescence in solution (λ_{max} = 339 nm), and is indicative of tryptophan emission from a more hydrophobic environment, which nonetheless contains some water. The efficiency of aqueously soluble acrylamide quenching also argues for water at or near the interfacial region. In addition, calculations of the probability of α-helix formation and the helical hydrophobic moment (Pownall et al., 1983) in apo A-I show that the four tryptophan residues occur on the hydrophobic faces (high helical hydrophobic moments) of amphiphilic helices. Figure 7 shows the location of the four tryptophan residues of apo A-I in helical wheel representations. The resolved helical hydrophobic moment (vector arrow) in Figure 7 determines the orientation of the amphiphilic helix, relative to the lipid surface. The midpoint of the vector arrow coincides with the midpoint of the helical axis. The shaded area of the arrow represents the nonpolar projection of the helical hydrophobic moment and determines the depth of penetration of the helix into the lipid matrix, whereas the unshaded area corresponds to the helical face solubilized by the aqueous phase. The confluence of the shaded and unshaded regions of the vector arrow dictates the placement of the α-helix at the lipid–protein interface. In apo A-I two of the tryptophan residues (8, 72) occur at the edge of the interface, and the other two tryptophans (50, 108) lie on the nonpolar face of the amphiphilic helix. A similar analysis for apo C-I (Segrest et al., 1983) and apo C-II (data not shown) shows that the tryptophan residues of each protein fall at the lipid–protein interface. We submit that differences in oxygen quenching parameters between apo A-I and apo C in recombinant HDL may occur because of variations in tryptophan placement, relative to the lipid–protein interface.

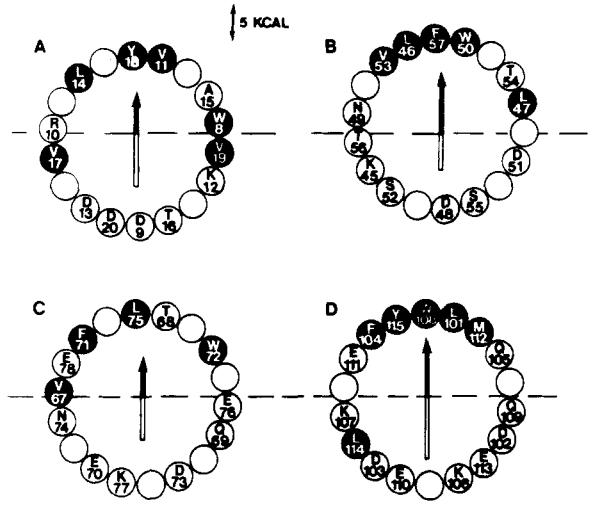

FIGURE 7: Helical wheel representation of apo A-I sequence regions, which contain tryptophan. Nonpolar residues are presented in shaded circles. The vector arrow in the center represents the helical hydrophobic moment and points in the nonpolar direction. The shaded portion of the arrow represents the nonpolar component of the moment, and the unshaded portion corresponds to the polar component. The arrow length expresses energy in kcal. The confluence of shaded and unshaded regions of the arrow establishes the depth of helical penetration into the lipid matrix. The lipid–water interface is represented by the dashed horizontal line. The four helical regions presented are as follows: panels A (residues 8–20), B (residues 45–57), C (residues 67–78), and D (residues 101–115).

The temperature dependence and relative efficiency of our acrylamide quenching of DMPC/apo A-I intrinsic fluorescence intensity (Figure 6, panel A) is consistent with the concepts of (a) bound water at the interface (Massey et al., 1985) and (b) increased hydration accompanying phospholipid melting (Table II). The oxygen quenching data of DMPC/apo A-I fluorescence (Figure 4), as evaluated by our two-compartment model, also support the hydrated interface concept. The measured apparent k^* actually represents the number of effective quenching collisions per unit time per unit volume, and these values are subsequently converted to diffusion parameters by application of Smoluchowski's original theory for bimolecular reactions. For an oxygen quencher molecule, originating in the hydrocarbon phospholipid domain, to effectively quench a tryptophan residue at the interface, near the hydrated

phospholipid carbonyl moiety, it must first diffuse through the lipid phase and then overcome an activation barrier for solvation. The strong temperature dependence of fluorescence quenching by oxygen in the recombinant HDL may incorporate not only oxygen partition terms (eq 8) but also an oxygen solvation barrier. Since proteins are dynamic systems with many substrates oscillating around an average conformation, a type of dynamic gate (open and closed pathway) to solvation may exist (Beece et al., 1980). Such an interfacial solvation barrier could account for part of the disproportionately large difference in $k'_q(T)$ between the DMPC/apo A-I (Table I and eq 8) and DMPC/apo C (Maliwal et al., 1985) complexes, described in the preceding section. A physical basis for this difference may arise from variations of amphiphilic α-helix penetration into the phospholipid matrix (contrast acyl and carbonyl regions) or a shift in the position of the tryptophan residue in the α-helix, relative to the helical hydrophobic moment (Pownall et al., 1983), as discussed in the preceding paragraph (Figure 7). The reduction in the temperature dependence of the oxygen quenching efficiency by the addition of sucrose (Table I), which tends to dehydrate the phospholipid–water interface, could reflect changes in such a solvation barrier rather than solely mechanical, viscosity considerations.

Conclusions

The surface of lipoproteins, which generally consists of a protein–phospholipid–water interface, is critical for the proper function of physiologically important events such as the action of lipid transfer proteins or lecithin:cholesterol acyltransferase, or the binding and displacement of surface-active proteins like apo A and apo C. Our fluorescence quenching studies are consistent with observations in recombinant HDL, containing apo A-I and dimyristoylphosphatidylcholine, indicating that the interfacial region is hydrated and the dynamics of small molecule quenchers, like oxygen or acrylamide, are affected by interfacial properties. We have introduced a two-compartment model (aqueous and lipid phases) to analyze our quenching data. The temperature dependence of the quenching rates reflects differences in quencher concentrations (in each compartment) and perhaps diffusion constants, rather than gross apo A-I conformational changes (e.g., increased α-helix formation) related to lipid binding. Comparison of our oxygen quenching data on DMPC/apo A-I complexes with that on DMPC/apo C suggests the importance of (a) the location of tryptophan relative to the interface as modeled by amphiphilic moment calculations and (b) an oxygen solvation barrier at the protein–phospholipid interface. In lipid-free form, our apo A-I fluorescence intensity and lifetime quenching data, for both oxygen and acrylamide, show that rapid, small-amplitude protein fluctuations necessary for quencher diffusion are inefficient even though the free energy of apo A-I denaturation, which occurs on a slower time scale (W. W. Mantulin, unpublished results), is low. Finally, our studies provide a more refined description of the protein dynamics of lipid-associating proteins and thus enhance our understanding of the properties of these physiologically important proteins.

Acknowledgments

We thank Drs. Weber, Reinhart, and Eftink for access to their fluorescence lifetime instrumentation and for thought-provoking discussions during the course of these studies. We acknowledge the artwork created by Susan Kelley and the manuscript preparation of Dottie Tullos.

Registry No. O_2, 7782-44-7; acrylamide, 79-06-1; sucrose, 57-50-1.

References

Baker, H. D., Delahunty, T., Gotto, A. M., Jr., & Jackson, R. L. (1974) *Proc. Natl. Acad. Sci. U.S.A. 71*, 3631.

Bartlett, D. R. (1959) *J. Biol. Chem. 234*, 466.

Beece, D., Eisenstein, L., Frauenfelder, H., Good, D., Marden, M. C., Reinisch, L., Reynolds, A. H., Sorenson, L. B., & Yue, K. T. (1980) *Biochemistry 19*, 5147.

Beechem, J. M., & Brand, L. (1985) *Annu. Rev. Biochem. 54*, 43.

Brewer, H. B., Jr., Fairwell, T., LaRue, A., Ronan, R. Houser, A., & Bronzert, T. J. (1978) *Biochem. Biophys. Res. Commun. 80*, 623.

Brouillette, C. G., Jones, J. L., Ng, T. C., Kercret, H., Chung, B. H., & Segrest, J. P. (1984) *Biochemistry 23*, 359.

Chowdry, B. Z., Lipka, G., & Sturtevant, J. M. (1984) *Biophys. J. 46*, 419.

Dvorin, E., Mantulin, W. W., Rohde, M. F., Gotto, A. M., Jr., Pownall, H. J., & Sherrill, B. C. (1985) *J. Lipid Res. 26*, 38.

Edelhoch, H. (1967) *Biochemistry 6*, 1948.

Edelstein, C., & Scanu, a. M. (1980) *J. Biol. Chem. 255*, 5747.

Eftink, M. R., & Ghiron, C. A. (1976) *J. Phys. Chem. 80*, 486.

Eftink, M. R., & Ghiron, C. A. (1981) *Anal. Biochem. 114*, 199.

Eftink, M. R., & Jameson, D. M. (1982) *Biochemistry 21*, 4443.

Eisenberg, D., Weiss, R. M., & Terwilliger, T. C. (1982) *Nature (London) 299*, 371.

Gratton, E., & Limkeman, M. (1983) *Biophys. J. 44*, 315.

Jackson, R. L., Morrisett, J. D., Sparrow, J. T., Segrest, J. P., Pownall, H. J., Smith, L. C., Hoff, H. F., & Gotto, A. M., Jr. (1974) *J. Biol. Chem. 249*, 5314.

Jameson, D. M., Gratton, E., Weber, G., & Alpert, B. (1984) *Biophys. J. 45*, 795.

Jonas, A., Privat, J. P., Wahl, P., & Osborne, J. C., Jr. (1982) *Biochemistry 21*, 6205.

Krebs, K. E., & Phillips, M. C. (1983) *Biochim. Biophys. Acta 754*, 227.

Lakowicz, J. R. (1982) in *Hemoglobin and Oxygen Binding* (Chien, H., Ed.) p 443, Elsevier North-Holland, Amsterdam.

Lakowicz, J. R., & Weber, G. (1973) *Biochemistry 12*, 4171.

MacDonald, R. I. (1985) *Biochemistry 24*, 4058.

Maliwal, B. P., Cardin, A. D., Jackson, R. L., & Lakowicz, J. R. (1985) *Arch. Biochem. Biophys. 236*, 370.

Mantulin, W. W., & Pownall, H. J. (1983) in *Excited States of Biopolymers* (Steiner, R. F., Ed.) p 163, Plenum, New York.

Mantulin, W. W., & Pownall, H. J. (1985) *Biochim. Biophys. Acta 836*, 215.

Mantulin, W. W., Rhode, M. F., Gotto, A. M., Jr., & Pownall, H. J. (1980) *J. Biol. Chem. 255*, 8185.

Mantulin, W. W., Massey, J. B., Gotto, A. M., Jr., & Pownall, H. J. (1981) *J. Biol. Chem. 256*, 10815.

Massey, J. B., She, H. S., & Pownall, H. J. (1985) *Biochemistry 24*, 6973.

Matz, C. D., & Jonas, A. (1982) *J. Biol. Chem. 257*, 4535.

Morrisett, J. D., Jackson, R. L., & Gotto, A. M., Jr. (1977) *Biochim. Biophys. Acta 472*, 93.

Parker, C. A. (1968) in *Photoluminescence of Solutions*, p 220, Elsevier, New York.

Peters, A., & Kimmich, R. (1978) *Biophys. Struct. Mech. 4*, 67.

Pownall, H. J., & Smith, L. C. (1974) *Biochemistry 13*, 2590.

Pownall, H. J., Massey, J. B., Kusserow, S. K., & Gotto, A. M., Jr. (1978) *Biochemistry 17*, 1183.
Pownall, H. J., Pao, Q., Hickson, D., Sparrow, J. T., Kusserow, S. K., & Massey, J. B. (1981a) *Biochemistry 20*, 6630.
Pownall, H. J., Hickson, D., & Gotto, A. M., Jr. (1981b) *J. Biol. Chem. 256*, 9849.
Pownall, H. J., Knapp, R. D., Gotto, A. M., Jr., & Massey, J. B. (1983) *FEBS Lett. 159*, 17.
Reijngoud, D.-J., & Phillips, M. C. (1984) *Biochemistry 23*, 276.
Rosseneu, M., vanTornout, P., Lievens, M.-J., Schmitz, G., & Assmann, G. (1982) *Eur. J. Biochem. 128*, 455.
Scanu, A. M., Edelstein, C., & Shen, B. W. (1982) in *Lipid–Protein Interactions* (Jost, P., & Griffith, O. H., Eds.) p 259, Wiley-Interscience, New York.
Segrest, J. P., Jackson, R. L., Morrisett, J. D., & Gotto, A. M., Jr. (1974) *FEBS Lett. 38*, 247.
Segrest, J. P., Chung, B. H., Brouillette, C. G., Kanellis, P., & McGahan, R. (1983) *J. Biol. Chem. 258*, 2290.
Soutar, A. K., Garner, C. W., Baker, H. N., Sparrow, J. T., Jackson, R. L., Gotto, A. M., Jr., & Smith, L. C. (1975) *Biochemistry 14*, 3057.
Subczynski, W. K., & Hyde, J. S. (1983) *Biophys. J. 41*, 283.
Subczynski, W. K., & Hyde, J. S. (1984) *Biophys. J. 45*, 743.
Tall, A. R., Shipley, G. G., & Small, D. M. (1976) *J. Biol. Chem. 251*, 3749.
Tall, A. R., Small, D. M., Deckelbaum, R. J., & Shipley, G. G. (1977) *J. Biol. Chem. 252*, 2200.
Vaughn, W. M., & Weber, G. (1970) *Biochemistry 9*, 464.
Washburn, E. W., Ed. (1928) in *International Critical Tables*, 1st ed., Vol. 3, pp 257 and 272, McGraw-Hill, New York.
Watts, A., Marsh, D., & Knowles, P. F. (1978) *Biochemistry 17*, 1792.
Weber, G., & Farris, F. J. (1979) *Biochemistry 18*, 3075.
Weinberg, R. B., & Spector, M. S. (1985) *J. Biol. Chem. 260*, 4914.
Zacchariasse, K. A., Phuc, N. V., & Kozankiewicz, B. (1981) *J. Phys. Chem. 85*, 2676.

Role of Free Radical Processes in Stimulated Human Polymorphonuclear Leukocytes†

Michael J. Thomas,* Pamela S. Shirley, Catherine C. Hedrick, and Lawrence R. DeChatelet
Department of Biochemistry, Bowman Gray School of Medicine of Wake Forest University, Winston-Salem, North Carolina 27103

Received December 31, 1985; Revised Manuscript Received June 23, 1986

ABSTRACT: Human polymorphonuclear leukocytes produce large quantities of superoxide when they attack and kill bacteria. However, superoxide is a weak oxidizing and reducing agent, and other more reactive oxygen species derived from reactions of superoxide are suggested to participate in the killing processes. To test the hypothesis that a reactive free radical or singlet oxygen is involved in bactericidal activity, human polymorphonuclear leukocytes were exposed to phagocytozable particles containing lipids that contain the easily autoxidized 1,4-diene moiety. After incubation the preparations were extracted and the extracts reduced with $NaBH_4$ to convert hydroperoxides to stable alcohols. Using gas chromatography/mass spectrometry to analyze the extracts, we were unable to detect products unless iron salts were added to the medium. The products obtained by extraction are those that would be expected if both free radical chain autoxidation and $^1O_2$ oxidation were taking place. In summary, we find that polymorphonuclear leukocytes do not cause peroxidation, implying that formation of strongly oxidizing free radicals is not an intrinsic property of the leukocyte. Added iron catalyzes peroxidation by activated leukocytes yielding an unusual distribution of hydroxylated products.

The human polymorphonuclear leukocyte (PMNL)[1] generates large quantities of superoxide and its disproportionation product H_2O_2 when it attacks bacteria. That the generation of these oxidants is essential for killing bacteria is implicit from studies on patients that suffer from chronic granulomatous disease (CGD). Characteristic traits of the CGD PMNL are the inability to produce superoxide (Curnutte et al., 1974) and the inability to kill phagocytozed bacteria (Quie et al., 1967; Kaplan et al., 1968). Because superoxide is both a weak oxidant and reductant (Sawyer & Valentine, 1981), other species have been sought as the agents responsible for killing. Several reports have suggested that singlet oxygen ($^1O_2$) (Rosen & Klebanoff, 1977) and hydroxyl radical (HO•) (Johnston et al., 1975; Tauber & Babior, 1977; Ambruso & Johnston, 1981; Sagone, 1981; Newburger & Tauber, 1982) are formed by reactions requiring superoxide or its disproportionation product H_2O_2. Recent studies on $^1O_2$ formation from superoxide disproportion have shown that this pathway is not operating to a significant extent (Foote et al., 1980a), and attempts to detect $^1O_2$ in the PMNL phagosome have been unsuccessful (Foote et al., 1980b).

† This work was supported by Research Grants GM29611 and AI10732 from the National Institutes of Health.
* Author to whom correspondence should be addressed.

[1] Abbreviations: BHT, 2,6-di-*tert*-butyl-4-methylphenol; BSA, bovine serum albumin; CGD, chronic granulomatous disease; CML, carboxy-modified latex; GC/MS, gas chromatography/mass spectrometry; DMPO, 5,5-dimethyl-1-pyrroline *N*-oxide; DMPO-OH, 2,2-dimethyl-5-hydroxypyrrolidinyl-1-oxy; DMPO-OOH, 2,2-dimethyl-5-hydroperoxy-pyrrolidinyl-1-oxy; H•, hydrogen atom; HO•, hydroxyl radical; HO_2•, perhydroxyl radical; HPLC, high-pressure liquid chromatography; HMS, hexose monophosphate shunt; NEM, *N*-ethylmaleimide; NHE, normal hydrogen electrode; $^1O_2$, singlet oxygen ($^1\Delta_g$); PBS, Dulbecco's phosphate-buffered saline; PMNL, polymorphonuclear leukocyte; SOD, superoxide dismutase.

0006-2960/86/0425-8042$01.50/0